

1 **Improving efficiency and sustainability of chitin bioconversion through a combination of**
2 ***Streptomyces secretomes* and mechanical-milling**

3
4 Lal Duhsaki, Saumashish Mukherjee and Jogi Madhuprakash*

5 Department of Plant Sciences, School of Life Sciences, University of Hyderabad,
6 Gachibowli, Hyderabad-500046, Telangana, India.

7
8
9
10
11
12
13
14
15
16
17
18
19
20
21
22
23
24
25
26
27
28 ***Author for correspondence:**

29 Dr. Jogi Madhuprakash
30 Department of Plant Sciences
31 School of Life Sciences
32 University of Hyderabad
33 Prof. CR Rao Road, Gachibowli,
34 Hyderabad-500046, India
35 Tel: +91-40-23134566
36 Fax: +91-40-23010120
37 E-mail: jmpsl@uohyd.ac.in

38 ABSTRACT

39 Chitin, particularly α -chitin, is the most abundant and highly recalcitrant form, fortified by an
40 intricate network of hydrogen bonds. Efficient valorization of α -chitin requires a mild pre-
41 treatment and enzymatic hydrolysis. *Streptomyces* spp. secrete chitin-active CAZymes that can
42 efficiently tackle the recalcitrant problem of chitin biomass. To better understand the potential
43 of *Streptomyces* spp., a comparative analysis was performed between the novel isolate,
44 *Streptomyces* sp. UH6 and the well-known chitin degraders, *S. coelicolor* and *S. griseus*.
45 Growth studies and FE-SEM analysis revealed that all three *Streptomyces* spp. could utilize
46 and degrade both α - and β -chitin. Zymogram analysis showed expression of 5-7 chitinases in
47 the secretomes of *Streptomyces* strains. The chitin-active-secretomes produced by
48 *Streptomyces* sp. UH6 and *S. griseus* were optimally active at acidic pH (pH 4.0 and 5.0) and
49 50°C. Time-course degradation of α - and β -chitin with the secretomes generated *N*-acetyl-*D*-
50 glucosamine (GlcNAc) and *N,N*-diacetylchitobiose [(GlcNAc)₂] as the predominant products.
51 Further, the highly crystalline α -chitin was subjected to pre-treatment by ball-milling, which
52 reduced the crystallinity from 88% to 56.6% and increased the BET surface area by 3-folds.
53 Of note, the activity of all three *Streptomyces* secretomes was improved by a mild pre-
54 treatment, while *Streptomyces* sp. UH6 secretome displayed improved GlcNAc and (GlcNAc)₂
55 yields by 14.4 and 9.6-folds, respectively. Overall, our results suggest that the *Streptomyces*
56 chitin-active-secretomes, particularly *Streptomyces* sp. UH6, can be deployed for efficient
57 valorization of chitin biomass and to establish an economically feasible and eco-friendly
58 process for valorizing highly recalcitrant α -chitin.

59

60 **Keywords:** α -Chitin, *Streptomyces*, Chitin-Active-Secretome, Ball-Milling, (GlcNAc)₁₋₂

61

62 1. INTRODUCTION

63 Chitin is a naturally occurring homopolymer consisting of *N*-acetyl-*D*-glucosamine (GlcNAc)
64 monomers linked together by β -1,4-glycosidic bonds. It is the second most abundant
65 biopolymer found in nature, surpassed only by cellulose. Chitin plays a crucial structural role
66 in the exoskeleton of arthropods and crustaceans, as well as in the cell wall of fungi.¹ Chitin
67 biomass can be processed through mechanical, chemical or biological means (via microbes or
68 enzymes) to produce chitooligosaccharides (CHOS). CHOS are highly sought-after
69 commercially due to their biodegradable, biocompatible, and non-toxic properties.² The
70 monosaccharide GlcNAc and disaccharide, *N,N*-diacetylchitobiose [(GlcNAc)₂] are
71 particularly important among CHOS, owing to their diverse biological applications. GlcNAc

72 is widely used in medicine for its anti-bacterial, anti-oxidant, and anti-tumor properties, and as
73 a clinical drug for rheumatism and rheumatoid arthritis.³ It can also promote the synthesis of
74 synovial fluid and increase skin hyaluronic acid content.³ Further, it is also used as food
75 additive and for seed treatments and foliar applications in agriculture.³ Of note, GlcNAc is also
76 used in the production of various valuable nitrogen-containing chemicals.³ (GlcNAc)₂ or
77 chitobiose, on the other hand, has been shown to have implications in medicine and
78 therapeutics, such as protection against acute hepatotoxicity induced by CCl₄-induced,⁴ high
79 anti-oxidant and DNA protection activities,⁵ amelioration of metabolic dysfunction in type 2
80 diabetes mice,⁶ and alleviation of oleic acid-induced lipid accumulation.⁷ Given the diverse
81 commercial applications of GlcNAc and chitobiose, it is imperative to maximize their
82 production through efficient and sustainable chitin valorization approaches.

83 However, the main obstacle for efficient valorization of chitin biomass is its high
84 crystallinity and resistance to degradation due to other intimate contaminants. Chitin occurs
85 naturally in two primary polymorphic forms, α - and β -chitin, with the former being the most
86 prevalent and crystalline form. The high degree of crystallinity in α -chitin is due to two factors:
87 tightly packed alternating parallel and anti-parallel chains and the presence of both inter- and
88 intra-sheet hydrogen bonds.^{1, 8} While employing enzymatic methods for α -chitin valorization
89 is environmentally friendly, the enzyme load required to facilitate efficient hydrolysis would
90 be substantial, resulting in high process costs. To overcome this limitation and develop new
91 technologies for efficient chitin valorization, integrated approaches such as mechano-
92 enzymatic,⁹ chemo-enzymatic¹⁰ or a combination both are in high demand. These approaches
93 mainly involve mild pre-treatment of crystalline chitin using mechanical (such as milling) or
94 chemical (such as ionic liquids) methods, followed by enzymatic hydrolysis to improve overall
95 CHOS yields, particularly GlcNAc and (GlcNAc)₂.^{9, 10}

96 Ball-milling is a dry mechanical method used to amorphize crystalline chitin substrates.
97 In ball-milling, the substrate is mixed with balls of varying sizes (made of high hardness
98 materials such as zirconium or stainless steel) in a specific ratio within a sealed chamber. The
99 chamber rotates at a set rpm, leading to a reduction in particle size and crystallinity of the
100 substrate due to frictional impact between the substrate, the balls, and the chamber walls.¹¹
101 Although there are reports of using a combination of ball-milling and enzymatic hydrolysis
102 (mainly with mono-component enzymes),^{9, 12} it would be interesting to investigate the
103 effectiveness of this method when using the “chitin-active-secretomes” of microbial origin.
104 Employing such chitin-active-secretomes (rich in chitin-active CAZymes) will avoid the costs
105 associated with producing mono-component recombinant enzymes.

106 When considering sustainability and environmentally friendly methods, biological,
107 specifically enzyme-catalyzed chitin degradation is the most preferred approach. In nature,
108 microorganisms, particularly bacteria, degrade chitin using chitinolytic enzymes for nutrition.
109 Enzymatic chitin degradation involves a synergistic interplay between different chitinolytic
110 enzymes, such as lytic polysaccharide monooxygenases (LPMOs), chitinases, and β -N-
111 acetylglucosaminidases.^{9, 13-15} *Streptomyces*, the largest genus in the phylum Actinobacteria, is
112 gram-positive and can degrade complex polysaccharides, including chitin and thus play a key
113 role in the nature's carbon cycle.^{16, 17} In general, *Streptomyces* harbours genomes of larger size
114 (>5 Mb), which encode a plethora of carbohydrate-active enzymes (CAZymes) for degradation
115 of complex polysaccharides.¹⁷ Among the known *Streptomyces* species, chitinolytic enzymes
116 from *S. coelicolor*¹⁸⁻²¹ and *S. griseus*,^{14, 22, 23} have been well-studied. Recently we reported
117 *Streptomyces* sp. UH6, a novel strain isolated from the University of Hyderabad campus, has a
118 promising chitin-degrading/modifying enzyme machinery.¹⁷ The genome of *Streptomyces* sp.
119 UH6 comprises a diverse range of chitin-active CAZymes, including five chitinases (four
120 GH18 and one GH19), four AA10 LPMOs, and four β -N-acetylglucosaminidases (four GH20
121 and one GH3).¹⁷ The secretome of *Streptomyces* sp. UH6 showed high activity towards highly
122 crystalline chitin substrates, indicating the potential for efficient valorization of such
123 substrates.¹⁷ Further, exploration of the *Streptomyces* sp. UH6 'chitin-active-secretome' could
124 yield valuable insights into chitin degradation and its applications.

125 In this study, we investigated the chitinolytic potential of *Streptomyces* sp. UH6,
126 compared to the well-studied *Streptomyces* spp., *S. coelicolor* and *S. griseus*. Growth and
127 chitinase activity studies confirmed the ability of all the three *Streptomyces* spp. to effectively
128 utilize chitin biomass, and field emission-scanning electron microscopy (FE-SEM) analysis
129 confirmed the deformations in chitin particles. On the other hand, zymogram analysis
130 confirmed the expression of chitinase isozymes in the 'chitin-active-secretomes' of the
131 *Streptomyces* spp. Time-course degradation of α - and β -chitin was performed to understand the
132 CHOS profile and overall yields generated. Further, the α -chitin substrate was subjected to pre-
133 treatment by ball-milling and the milled substrates were characterized to understand the
134 changes in physical properties after pre-treatment. Additionally, the milled substrates were
135 subjected to hydrolysis using the secretomes of *Streptomyces* spp., thereby confirming our
136 hypothesis that 'chitin-active-secretomes' can be effectively utilized for chitin biomass
137 valorization.

138
139

140 2. EXPERIMENTAL

141 2.1. Bacterial strains, chemicals and reagents

142 *Streptomyces* sp. UH6 was isolated from soil samples collected at the University of Hyderabad
143 campus located in Hyderabad, India at coordinates 17°27'22"N, 78°18'54"E.¹⁷ While, the
144 strains, *Streptomyces griseus* DSM 40236 and *Streptomyces coelicolor* A3(2) were procured
145 from DSMZ (Braunschweig, Germany). Both α - and β -chitin were purchased from Mahtani
146 Chitosan, located in Gujarat, India. Colloidal and glycol chitin were prepared as previously
147 reported.² All chemicals and reagents were purchased from HiMedia Laboratories and Sisco
148 Research Laboratories Pvt. Ltd., Mumbai, India, unless otherwise specified.

149 2.2. Growth of *Streptomyces* species on α - and β - chitin substrates

150 To investigate chitin utilization, the three *Streptomyces* species were cultured in M9 minimal
151 media containing 47.7 mM Na₂HPO₄, 22 mM KH₂PO₄, 8.5 mM NaCl, 9.4 mM NH₄Cl, 1 mM
152 MgSO₄ and 0.3 mM CaCl₂. The media was enriched with 1X trace elements and vitamins (1
153 mM each of biotin and thiamine) and supplemented with 0.5% α - or β -chitin as the sole carbon
154 source. Prior to the main experiment, each *Streptomyces* species was pre-cultured in R-2A
155 broth for 48h at their optimal growth temperatures. Later, the fully grown cultures were
156 harvested and washed with sterile milliQ water and resuspended in 1X M9 medium. The optical
157 density of the resuspended cultures was measured at 600 nm and adjusted to 0.1. A 1%
158 inoculum was added to the chitin containing minimal media and cultured at their respective
159 optimal growth temperatures. Samples were collected at different time points over a 10-day
160 period to estimate the total cellular protein, which is an indicator of growth, and extracellular
161 chitinase activity. All experiments were conducted in biological triplicates.

162 2.2.1. Estimation of total cellular protein

163 Growth of the *Streptomyces* spp. on different forms of chitin substrates was examined by
164 estimating the total cellular protein from the culture pellet collected at different time points as
165 reported previously.² To these cell pellets, 0.2N NaOH was added and boiled at 120°C for 10
166 min to lyse the cells. This was followed by centrifugation at 12000 rpm for 15 min at 4°C, and
167 the total cell protein was estimated using standard Bradford's method, as instructed in the
168 manufacturer's protocol (Sigma Aldrich, USA).

169 2.2.2. Estimation of chitinase activity for the secretomes

170 Chitinase activity was measured by Schales' assay as described earlier²⁴, with slight
171 modifications. A 200 μ L of reaction mixture consisting of 50 mM sodium acetate pH 5.5, 0.5%
172 colloidal chitin and 50 μ L culture supernatant was incubated for 1 h at 37°C and 800 rpm
173 shaking. The samples were centrifuged at 10000 rpm for 15 min at 4°C and 100 μ L of the

174 supernatant was boiled with 300 μ L Schales' reagent (0.5 M sodium carbonate and 0.5 g/L
175 potassium ferricyanide). Absorbance was measured at 420 nm. Quantification of reducing
176 sugars was done using a GlcNAc standard curve. One unit of enzyme activity was defined as
177 the amount of enzyme that liberated 1 μ mol of reducing sugar per hour.

178 **2.3. FE-SEM analysis to track deformities in chitin flakes**

179 Direct visualization of α - and β -chitin degradation by the three *Streptomyces* species was
180 performed using FE-SEM. Sample preparation protocol and FE-SEM analysis parameters were
181 maintained similar to those reported by Mukherjee et al., (2020)², with slight modifications.
182 For each strain, three experimental setups were created, including two control setups with
183 untreated α - and β -chitin separately, and one test setup with *Streptomyces* spp. grown in M9-
184 minimal media supplemented with α - or β -chitin at their optimal growth temperatures. Samples
185 were collected for FE-SEM analysis at 96 h and 72 h for α - and β -chitin, respectively. All
186 samples were harvested by centrifugation at 10,000 rpm for 3 min at 4°C, resuspended in 2.5%
187 glutaraldehyde, and incubated at 4°C overnight for pre-fixation. The samples were then
188 dehydrated using a progressive ethanol washing (10, 30, 50, 70, 90 and 100% [v/v]) and placed
189 on a clean glass coverslip attached to two-sided magnetic tape on a stub. A single chitin flake
190 (untreated or treated) was analyzed using Quorum Q150T ES sputter, and gold coating was
191 done for 120 s before FE-SEM analysis was performed using the Merlin Compact (model no.
192 20-59) of Carl Zeiss, Germany. The parameters for high resolution imaging were set at working
193 distance of 2-20 μ m and 5 and 3 kV accelerating voltage, and the magnification range varied
194 from 500-10,000X.

195 **2.4. Semi-native PAGE analysis of secretomes to identify chitin-active CAZymes**

196 The secretomes of the three different *Streptomyces* spp. under investigation were collected over
197 α - and β - chitin, at their respective optimal activity times. To visualize the chitinase isozymes
198 in the secretome fractions, a zymogram analysis was performed using 12% SDS-PAGE
199 containing 2.5% glycol chitin. A 10 μ L sample of culture supernatant was mixed with 4 μ L of
200 loading dye (1M Tris-HCl pH 6.8, 10% SDS, 50% Glycerol, 0.05% bromophenol blue and
201 14.3 M β -mercaptoethanol) and boiled at 80°C for 10 min before electrophoresis. Analysis was
202 conducted on samples collected from at least three different experiments. After electrophoresis,
203 the gels were washed at least three times with 50 mM Tris Cl (pH 8.0) containing 0.1% Triton
204 X-100 and twice with 50 mM Tris Cl (pH 8.0) and then incubated in the same buffer at 37°C
205 overnight. The gels were stained with Calcofluor-white M2R dye (Sigma Aldrich, USA) for
206 20 min and washed thoroughly with double distilled water before examination for the presence
207 of bands under UV transilluminator.

208 **2.5. Determination of optimal conditions for efficient saccharification**

209 *Streptomyces* spp. were grown in M9-minimal medium with 0.5% β -chitin until peak chitinase
210 activity was reached. The resulting secretomes were obtained by centrifugation at 8000 rpm
211 for 20 min at 4°C, and their concentration was measured by Bradford's method. The secretomes
212 were then stored at -20°C for subsequent characterization experiments.

213 **2.5.1. pH and temperature optima**

214 Optimal pH for the secretomes was determined using various 50 mM buffers within a pH range
215 of 2.2 to 10.0. The buffers used were glycine-HCl (pH 2.2-3.0), sodium citrate (pH 3.0-6.0),
216 sodium acetate (pH 4.0-5.5), sodium phosphate (pH 6.0-8.0), Tris-HCl (pH 7.2-9.0), and
217 glycine-NaOH (pH 9.0-10.0). Each reaction mixture contained a particular buffer and 50 μ L of
218 respective secretome, and was incubated with 0.5% colloidal chitin at 37°C and 800 rpm
219 shaking. Meanwhile, the optimal temperature for the secretomes was measured at a pH
220 determined in the previous experiment, with temperatures ranging from 10 to 80°C. Chitinase
221 activity was measured using Schales' assay as described the section 2.2.2, with all reactions
222 performed in triplicate and proper controls in place.

223 **2.5.2. Thermal stability of the chitin-active-secretomes**

224 Thermal stability experiments were performed at temperatures corresponding to the point of
225 maximal activity. The secretomes were subjected to incubation at 45°C and 50°C for various
226 time intervals, and the residual chitinase activity was measured using the Schales' assay as
227 described the section 2.2.2. To ensure accuracy, all reactions were conducted in triplicate and
228 included appropriate controls.

229 **2.6. Pre-treatment of shrimp shell α -chitin by ball-milling**

230 The shrimp shell α -chitin was subjected to pre-treatment through ball-milling using a SPEX
231 Sample Prep Mixer/Mill 8000 D. In this process, 2.5 g of α -chitin was mixed with 25 g of
232 stainless-steel balls of varying diameters, maintaining a ball to substrate ratio of 10:1. The
233 milling procedure was carried out for 30 and 60 min, respectively, at a speed of 1060 cycles
234 per min, resulting in the production of two milled powders named BM-30 and BM-60. The
235 structural properties of the α -chitin from shrimp shells were analyzed using various techniques
236 to assess the effects of ball-milling.

237 *Powder X-ray Diffraction (pXRD) analysis:*

238 The pXRD measurements were carried out on a PANalytical X'Pert³ powder diffractometer
239 using Cu-K α radiation with a wavelength of 1.54 Å, in a 2 θ range of 5°-40° and with a step size
240 of 0.0167°. The crystallinity index (I_{CR}) of the samples was calculated using the intensities of

241 the (110) and (I_{am}) peaks at 2θ values of $\sim 20^\circ$ (representing the maximum intensity) and $\sim 16^\circ$
242 (corresponding to the amorphous halo contribution), according to the following equation²⁵:

$$I_{CR} (\%) = [(I_{110} - I_{am})/I_{110}] \times 100$$

244
245 *Fourier Transform Infrared Spectroscopy (FTIR) analysis:*

246 The samples were uniformly compressed with KBr to create pellets/disks for FTIR analysis on
247 a PerkinElmer Frontier FTIR/FIR Spectrometer. The spectra were obtained using the
248 attenuated total reflection method and recorded in the range of 4000 cm^{-1} to 400 cm^{-1} .²⁵

249 *BET analysis:*

250 The surface area of the pre-treated chitin samples was determined using a surface area analyzer,
251 the Quantachrome autosorb iQ, Germany. The samples were subjected to degassing at 60°C for
252 24 h under a N_2 atmosphere to remove any moisture adsorbed on the solid surface. The specific
253 surface area was estimated using the BET surface area (S_{BET}) method.²⁵

254 **2.7. Time-course degradation of crystalline chitin substrates**

255 The time-dependent hydrolysis of crystalline chitin substrates, α - (native and pre-treated) and
256 β -chitin (10 mg/mL) was carried out using 5 U of chitin-active-secretomes. All reactions were
257 performed in triplicate under optimal conditions at 45°C and 1000 rpm. Aliquots were collected
258 at different time points between 1-72 h and filtered using a 96-well filter plate (0.45 μm filters;
259 Merck Millipore, USA) operated by a Millipore vacuum manifold. The products were analyzed
260 using HPLC (Shimadzu, Japan) equipped with Shim-pack GIST NH2 column (5 μm , 4.6 X
261 250, Shimadzu, Japan) at 210 nm, through isocratic elution with 70% acetonitrile at a flow rate
262 of 0.7 mL/min. The oligomers were identified and quantified using the respective CHOS
263 standards essentially as described previously.²⁶

264

265 **3. RESULTS & DISCUSSION**

266 In a previous study, we reported that the genome of *Streptomyces* sp. UH6 possessed a
267 complete chitin-active CAZyme repertoire.¹⁷ The isolate's ability to degrade various chitin
268 substrates, especially the crystalline chitin substrates α - and β -chitin, was also validated. The
269 chitinase activity on α - and β -chitin was found to be higher than that on colloidal chitin,
270 suggesting that the chitinolytic enzymes in the secretome of *Streptomyces* sp. UH6 prefer
271 highly crystalline chitin substrates. To gain deeper understanding of the chitinolytic potential
272 of *Streptomyces* sp. UH6, we performed a comparative study with two well-studied species, *S.*
273 *coelicolor* A3(2) and *S. griseus*.

274

275 **3.1. All three *Streptomyces* spp. were able to utilize crystalline chitin substrates**

276 The growth of the studied *Streptomyces* spp. was analyzed on M9 minimal medium
277 supplemented with α - and β -chitin as the sole carbon source. Samples were collected at regular
278 intervals up to 10 days to analyze the total cellular protein and extracellular chitinase activity.
279 *Streptomyces* sp. UH6 showed slower growth on α -chitin compared to β -chitin, with maximum
280 growth at 216 h and 96 h, respectively (Fig. 1A and B). *S. griseus* had similar growth rates on
281 α -chitin, but slower growth on β -chitin (maximum growth observed at 168 h). *S. coelicolor* had
282 the slowest growth among the three, with maximum growth at 240 h on both substrates.
283 Notably, *Streptomyces* sp. UH6 displayed the highest total cellular protein content at the peak
284 growth time point on both the substrates.

285 The extracellular chitinase activity followed the same pattern as growth studies, with
286 *Streptomyces* sp. UH6 exhibiting the highest activity on both the substrates (Fig. 1C and D).
287 However, activity on α -chitin was lower than on β -chitin, possibly due to the high crystalline
288 nature of α -chitin hindering chitinase accessibility and reducing saccharification efficiency.

289 **3.2. FE-SEM imaging of α - and β -chitin deconstruction by *Streptomyces* spp.**

290 FE-SEM visualization showed that *Streptomyces* sp. UH6, *S. coelicolor*, and *S. griseus*
291 colonized and perforated the surface of α - and β -chitin, resulting in de-fibrillation. While, the
292 untreated α -chitin displayed a smooth surface (Fig. 2A), the treated samples exhibited visible
293 colonization by the respective *Streptomyces* spp., accompanied by perforations and de-
294 fibrillation (Fig. 2B-D). The perforations and de-fibrillation were more intense in α -chitin for
295 *Streptomyces* sp. UH6 (Fig. 2B). β -chitin was degraded much faster and intensely by the
296 *Streptomyces* spp. While the untreated β -chitin had a smooth surface (Fig. S1A), dense
297 colonization of the strains and perforations were observed upon treatment (Fig. S1B-D),
298 leading to almost complete degradation at 96 h. Direct surface attachment and colonization
299 were the primary mechanism for crystalline chitin degradation, as observed in the FE-SEM
300 analysis, which is in agreement with the growth studies and previous findings with
301 *Paenibacillus* sp. LS1.²

302 **3.3. *Streptomyces* species can produce ‘chitin-active-secretomes’**

303 The secretomes produced by three *Streptomyces* spp., collected over α - and β -chitin, were
304 resolved using semi-native PAGE containing 2.5% glycol chitin, to understand the expression
305 pattern of different chitinase isozymes. For secretomes collected over α -chitin, six isozymes
306 were detected for *Streptomyces* sp. UH6, while *S. coelicolor* and *S. griseus* showed five and
307 four isozymes, respectively. In the case of secretomes collected over β -chitin, five isozymes
308 were observed for *Streptomyces* sp. UH6, while *S. coelicolor* and *S. griseus* displayed six and

309 seven isozymes, respectively. The isozymes detected were approximately within the range of
310 20-70 kDa (Fig. 3).

311 Previously, zymogram analysis of secretomes produced by *Paenibacillus* sp. LS1,
312 collected over different chitin substrates, revealed a higher expression of chitinase isozymes
313 on β - and colloidal chitin, as compared to α -chitin.² A similar observation was made in the
314 current study, where the expression of the chitinase isozymes was higher in β -chitin than α -
315 chitin for the secretomes produced by *Streptomyces* sp. UH6 and *S. griseus* (Fig. 3). However,
316 no significant difference in the expression of chitinase isozymes was observed on both
317 substrates for the secretome produced by *S. coelicolor*. The expression of six chitinase
318 isozymes on α -chitin by *Streptomyces* sp. UH6 indicates the potential of the isolate to utilize
319 recalcitrant forms of chitin.

320 **3.4. Biochemical characterization of the chitin-active-secretomes**

321 The process of chitin saccharification is greatly affected by reaction conditions, such as pH and
322 temperature. Therefore, to optimize the chitin valorization process and improve the production
323 of chitooligosaccharides, the influence of pH and temperature on the chitinase activity of the
324 secretomes produced by *Streptomyces* sp. UH6, *S. coelicolor*, and *S. griseus* was thoroughly
325 investigated.

326 **3.4.1. The chitin-active-secretomes were optimally active in acidic pH and 50°C**

327 The optimal pH for chitinase activity of the secretomes produced by *Streptomyces* sp. UH6, *S.*
328 *coelicolor* and *S. griseus* was investigated under different buffer conditions within the pH range
329 of 2-10 (Fig. 4A). The secretomes from *Streptomyces* sp. UH6 and *S. griseus* showed optimal
330 activity in 50 mM sodium acetate, pH 4.0, while the secretome from *S. coelicolor* was optimally
331 active at pH 5.0 of the same buffer (Fig. 4A). *Streptomyces* sp. UH6 secretome retained up to
332 70% activity throughout the acidic pH range of 2.0-6.0, while *S. griseus* secretome retained up
333 to 80% activity within the pH range of 5.0-7.0, with a sharp decline to $\leq 60\%$ at pH below 4.0.
334 Chitin-active-secretome from *S. coelicolor* retained up to $\sim 80\%$ was activity at pH 4.0, but a
335 sharp decline in activity was observed below pH 4.0 and above pH 5.0 (Fig. 4A).

336 All three chitin-active-secretomes showed optimal activity at 50°C (Fig. 4B). They
337 retained up to $\sim 90\%$ activity at 45°C and 55°C, except for *Streptomyces* sp. UH6 secretome,
338 which retained $\sim 80\%$ activity at 55°C (Fig. 4B). The optimal parameters observed for the
339 secretomes of *Streptomyces* spp. suggest the presence of chitinases that are active under acidic
340 conditions and could potentially promote efficient saccharification of chitin under such
341 conditions. It is noteworthy that similar observations were made in previous studies with
342 *Paenibacillus* sp. LS1 and *Aeromonas* sp. GJ-18, whose secretomes showed optimal activity

343 in 50 mM sodium acetate buffer, pH 4.0, and at 50°C and 10 mM sodium acetate buffer, pH
344 5.0, and 45°C, respectively.^{2, 27}

345 **3.4.2. The chitin-active-secretomes are relatively stable at 45°C**

346 The secretomes produced by *Streptomyces* sp. UH6 and *S. coelicolor* retained chitinase activity
347 up to 70% even after 120 min of pre-incubation at 45°C. Similarly, the secretome produced by
348 *S. griseus* retained up to 65% of chitinase activity under the same conditions (Fig. 4C).
349 However, at the optimal temperature of 50°C, *Streptomyces* sp. UH6 secretome retained up to
350 60% of chitinase activity upon pre-incubation up to 120 min. The secretome from *S. coelicolor*
351 was also stable at 50°C, retaining up to 70% activity after 120 min of pre-incubation (Fig. S2).
352 However, the secretome from *S. griseus* showed sharp decrease in activity, dropping to nearly
353 60% after only 20 min of pre-incubation at 50°C. The activity further decreased up to 50%
354 after 120 min of pre-incubation at 50°C (Fig. S2). Previously, secretome produced by
355 *Paenibacillus* sp. LS1 was reported to be stably active at 45°C, retaining up to 53% activity
356 after 90 min of pre-incubation, compared to its optimal temperature, 50°C where chitinase
357 activity declined up to 33% after only 20 min pre-incubation.² Our observations indicated that
358 the three secretomes were stably active at 45°C, and therefore all the further assays were
359 performed at this temperature.

360 **3.5. *Streptomyces* sp. UH6's chitin-active-secretome effectively breaks down chitin**

361 The ability of the three *Streptomyces* secretomes to degrade α - and β -chitin substrates was
362 compared over a time-dependant reaction. (GlcNAc)₂ was the primary product formed in all
363 three cases, followed by GlcNAc. Trace amounts of (GlcNAc)₃ and (GlcNAc)₅ were only
364 detected in case of reactions with *Streptomyces* sp. UH6 secretome (data not shown). From α -
365 chitin, the secretomes produced by *Streptomyces* sp. UH6, *S. coelicolor* and *S. griseus*
366 generated total CHOS [GlcNAc+(GlcNAc)₂] concentrations of 0.79 mM, 0.62 mM and 0.52
367 mM, respectively (Fig. 5A and B). Conversely, from β -chitin, the total CHOS generated were
368 6.2 mM, 4.2 mM and 2.9 mM, respectively (Fig. 5C and D). Notably, *Streptomyces* sp. UH6
369 secretome generated a higher concentration of CHOS from both crystalline chitin substrates
370 than the other two, indicating its efficiency in chitin biomass valorization. This can be
371 attributed to the chitinolytic enzyme machinery encoded by *Streptomyces* sp. UH6, which
372 comprises extracellularly secreted chitinases, β -N-acetyl-glucosaminidases and AA10 LPMOs
373 (those consisting of an N-terminal signal peptide).¹⁷ However, the low CHOS yields by the
374 *Streptomyces* secretomes from α -chitin can be attributed to the high crystallinity of the
375 substrate. Due to anti-parallel polymeric chain arrangements and intrinsic hydrogen bonding
376 within and among the polymeric chains, α -chitin, although most abundant yet recalcitrant form

377 of chitin.⁸ Hence, pre-treating α -chitin prior to enzymatic hydrolysis could be useful in
378 reducing the crystallinity of the substrate, and thereby enhancing the activity of chitin-active-
379 secretomes.

380 **3.6. The process of ball-milling induced alterations in the structure of α -chitin.**

381 To improve the substrate accessibility and enzymatic hydrolysis, α -chitin was pre-treated
382 through ball-milling. Typically, ball-milling breaks down the interchain hydrogen bond
383 network within chitin polymer, inducing alterations in the overall chitin structure and reducing
384 the polymer's crystallinity.³ The structural properties of the substrate before and after pre-
385 treatment were analyzed by FT-IR, pXRD and BET analysis and were compared between un-
386 milled α -chitin (UM α -chitin) and the two ball-milled substrates, BM-30 and BM-60. FT-IR
387 analysis revealed several changes in the spectra of the ball-milled substrates compared to the
388 UM α -chitin. The disappearance of a small peak between the wavenumbers 1619 and 1654 cm^{-1}
389 indicated loss of amide-I bond in the ball-milled substrates (Fig. 6A). Similar observations
390 were made in previous studies regarding changes in the 1640-1660 cm^{-1} region of the FT-IR
391 spectra after ball-milling chitin substrates.^{9, 12} Additionally, a flattening of the peak between
392 3259 and 3440 cm^{-1} indicated the loss of N-H and O-H stretching bonds, respectively (Fig.
393 6A). Furthermore, the decrease in peak intensity between 1029 and 1068 cm^{-1} indicated that
394 the ball-milling induced considerable breakage of the C-O stretching bonds, corresponding to
395 the glycosidic linkages in the chitin (Fig. 6B). Previously, loss of N-H and O-H stretching
396 bonds and C-O stretching bonds were observed for solid shrimp shell waste after ball-milling.²⁸
397 While several changes were observed in the spectral diagrams of the ball-milled substrates
398 compared to the UM α -chitin, these changes did not heavily distort the overall spectral sketch
399 of chitin.

400 The pXRD analysis revealed five crystal reflection peaks for all the substrates i.e., 020,
401 021, 110, 120 and 101 (Fig. 6C). Sharp peaks at $\sim 9^\circ$ (020) and $\sim 19^\circ$ (110) in the UM α -chitin
402 indicated a compact structure of the substrate, which is usually not accessible for direct
403 enzymatic hydrolysis. A significant decrease in the intensities of the above-mentioned peaks
404 was observed for both ball-milled substrates, with BM-60 showing the maximum decrease
405 (Fig. 6C). Further, the crystallinity index (C.I.) was calculated, revealing a substantial decrease
406 in the crystallinity of the milled chitin substrates. While UM α -chitin showed a C.I. of 88.3%,
407 the substrates BM-30 and BM-60 showed a decrease in the C.I. up to 72% and 56.6%,
408 respectively (Table 1). Previously, ball-milling powdery chitin for 4 h at 380 rpm led to a
409 decrease in C.I. from 86.9% to 52.2%.¹² In another study, a C.I. of 40% from 94% was achieved

410 for crab α -chitin, when ball-milled at 800 rpm for 30 min.⁹ However, in both cases, the authors
411 used of 10 mm diameter zirconia balls.

412 The BET surface areas (S_{BET}) of the resulting ball-milled chitin substrates were also
413 examined and compared against the UM α -chitin. The S_{BET} was 6.3, 10.6 and 18.6 m²/g for
414 UM, BM-30 and BM-60, respectively (Fig. 6D). This showed ~1.7 and 3-fold increase in
415 surface area for substrates BM-30 and BM-60, respectively, compared to UM α -chitin (Table
416 2). The increase in BET surface area could be due to the decrease in compactness of the α -
417 chitin structure as a result of hydrogen bond breakage between chitin chains by ball-milling.²⁹
418 Previously, shrimp chitin powder ball-milled for 60 min at 1060 cycles per minute had an S_{BET}
419 of 36.5 m²/g, however, the S_{BET} value for unmilled chitin was not provided.³⁰ The results
420 together indicate substantial changes in structural parameters of the UM α -chitin after pre-
421 treatment with ball-milling. These alterations in the chitin structure might be helpful in
422 promoting improved enzymatic hydrolysis by the *Streptomyces* chitin-active-secretomes.

423 **3.7 Pre-treatment of α -chitin with ball-milling enhanced its valorization by *Streptomyces*** 424 **chitin-active-secretomes**

425 With this study we compared CHOS production from ball-milled α -chitin substrates using
426 secretomes from the three *Streptomyces* species. The results showed that ball-milling followed
427 by enzymatic hydrolysis significantly increased both GlcNAc and (GlcNAc)₂ yields compared
428 to UM α -chitin. The secretome produced by *Streptomyces* sp. UH6 exhibited the most
429 significant hydrolytic activity. For example, the GlcNAc yield from UM α -chitin was only 0.32
430 mM after 72 h, whereas a substantial increase up to 1.6 mM was observed for BM-30 and up
431 to 4.6 mM for BM-60 (Fig. 7A). Similar observations were made for (GlcNAc)₂, which
432 increased from 0.47 mM to 2.3 mM and 4.5 mM from BM-30 and BM-60, respectively (Fig.
433 7B). These results suggest that ball-milling induces structural changes in α -chitin, such as
434 increased surface area and decreased crystallinity (particularly for BM-60), which improve the
435 hydrolytic efficiency of the chitin-active-secretomes produced by *Streptomyces* sp. UH6.

436 The secretomes produced by *S. coelicolor* and *S. griseus* also showed improvement in GlcNAc
437 and (GlcNAc)₂ yields from the ball-milled α -chitin substrates (Fig. 7C-F). However, the yield
438 obtained using the *Streptomyces* sp. UH6 chitin-active-secretome was higher compared to the
439 other two. Interestingly, the *Streptomyces* sp. UH6 chitin-active-secretome employed over
440 BM-60 produced nearly equal concentrations of both GlcNAc and (GlcNAc)₂ (4.6 mM and 4.5
441 mM, respectively), highlighting its clear advantage over the other two secretomes for efficient
442 hydrolysis of ball-milled α -chitin to produce value-added CHOS.

443 Previously, it was reported that ball-milling of crab α -chitin improved hydrolysis by
444 *Serratia marcescens* chitinases, both individually and in combination with *SmCBP21*.⁹ The
445 authors achieved up to 0.8 mM of (GlcNAc)₂ from the ball-milled crab α -chitin, compared to
446 less than 0.05 mM for the unmilled substrate after 48 h, resulting in almost a 16-fold increase
447 in yield. Additionally, combined hydrolysis of ball-milled powdery chitin by a chitinase and β -
448 *N*-acetylglucosaminidase from *P. barengoltzii* increased overall chitin conversion to GlcNAc
449 by 3.2-fold compared to the unmilled substrate.¹² While these studies utilized purified mono-
450 component enzymes, we used chitin-active-secretomes produced by *Streptomyces* species for
451 valorization of the α -chitin substrates, which makes our method economically feasible. We
452 found that the combination of BM-60 and chitin-active-secretome from *Streptomyces* sp. UH6
453 was the most preferred for enhanced production of both GlcNAc and (GlcNAc)₂ in equal
454 concentrations. Our results are comparable with the previously reported methods, with up to
455 14.4- and 9.6-fold higher GlcNAc and (GlcNAc)₂ yields, respectively from BM-60 compared
456 to the UM α -chitin using the chitin-active-secretome from *Streptomyces* sp. UH6.

457 Interestingly, while *S. griseus* and *S. coelicolor* A3(2) have a higher number of
458 chitinases and LPMOs in their CAZyme profiles compared to *Streptomyces* sp. UH6,¹⁷ the
459 latter is able to degrade both unmilled and milled α - and β -chitin much more efficiently. This
460 efficient chitin degradation by the chitin-active-secretome of *Streptomyces* sp. UH6 may be
461 attributed to the extracellular secretion of chitinases and LPMOs.¹⁷ According to the genome
462 analysis of *Streptomyces* sp. UH6, all the chitinases (both GH18 and GH19) and the LPMOs
463 encoded have an N-terminal signal peptide, indicating their extracellular secretion.¹⁷ Moreover,
464 the higher production of GlcNAc by the *Streptomyces* sp. UH6 secretome may be due to the
465 action of the β -*N*-acetylhexosaminidase containing a signal peptide (peg.2875). It could also
466 be possible that the chitinolytic enzymes produced by *Streptomyces* sp. UH6 are strong
467 degraders of chitin as compared to those secreted by *S. griseus* DSM 40236 and *S. coelicolor*
468 A3(2). However, further studies are needed to validate these observations through thorough
469 comparative molecular characterization of these chitin-active CAZymes.

470 **4. CONCLUSIONS**

471 A novel mechano-enzymatic approach that combines ball-milling with naturally produced
472 bacterial secretomes for bioconversion of crystalline α -chitin to GlcNAc and (GlcNAc)₂ has
473 been demonstrated. The ball-milling process significantly decreased the crystallinity and
474 increased the surface area of the normally compact α -chitin, enabling its enzymatic hydrolysis
475 with the secretome produced by *Streptomyces* sp. UH6 to produce both GlcNAc and (GlcNAc)₂

476 in equal concentrations. This eco-friendly method does not involve any harsh chemicals and is
477 cost-effective due to the use of naturally produced chitin-active-secretomes instead of mono-
478 component recombinant enzymes, which require expensive isolation and purification
479 procedures. Furthermore, this method could aid in the production of platform chemicals, such
480 as GlcNAc and (GlcNAc)₂ for various value-added products. *Streptomyces* sp. UH6's chitin-
481 active-secretome showed a clear advantage over those produced by *S. coelicolor* and *S. griseus*
482 in valorizing both unmilled and milled α -chitin as well as β -chitin, indicating the superior
483 efficiency of its chitin-active CAZymes. Despite encoding fewer chitin-active CAZymes in its
484 genome than *S. coelicolor* and *S. griseus*, *Streptomyces* sp. UH6 is a valuable target for chitin
485 valorization to GlcNAc and (GlcNAc)₂ on an industrial scale.

486

487 **ACKNOWLEDGEMENTS**

488 We extend our gratitude to Prof. Koteswararao V. Rajulapati of the School of Engineering
489 Sciences and Technology at the University of Hyderabad (UoH) for providing access to his
490 lab's ball-milling facility. Additionally, we would like to express our appreciation to the powder
491 XRD facility at the School of Physics, the FT-IR facility at ACRHEM, and the FE-SEM and
492 BET analysis facilities at the School of Chemistry, UoH, for their support in facilitating the
493 analysis of our chitin samples. LD would like to acknowledge UoH-BBL and UoH-IoE for the
494 fellowship. SM would like to thank Science and Engineering Research Board, GoI for the
495 fellowship.

496

497 **FUNDING SUPPORT**

498 The authors would like to express their gratitude to the Department of Science and Technology
499 (DST), Government of India (GoI), for the Funds for Infrastructure in Science and Technology
500 (FIST), Level II, as well as to the University Grants Commission supported Special Assistance
501 Programme (UGC-SAP-DRS-II) to the Department of Plant Sciences, UoH. The authors would
502 also like to thank the DBT-SAHAJ/BUILDER, (BT/INF/22/SP41176/2020) for their support
503 to School of Life Sciences, UoH. Furthermore, JM would like to acknowledge the funding
504 received from the Council of Scientific & Industrial Research, GoI (38(1503)/21/EMR-II),
505 Science and Engineering Research Board, GoI (CRG/2019/006426), and UoH-Institution of
506 Eminence (RC1-20-020).

507

508

509

510 REFERENCES

- 511 1. B. B. Aam, E. B. Heggset, A. L. Norberg, M. Sørli, K. M. Vårum and V. G. Eijsink,
512 *Mar. Drugs*, 2010, **8**, 1482-1517.
- 513 2. S. Mukherjee, P. K. Behera and J. Madhuprakash, *Carbohydr. Polym.*, 2020, **250**,
514 116889.
- 515 3. S. Cao, Y. Liu, L. Shi, W. Zhu and H. Wang, *Green Chem.*, 2022, **24**, 493-509.
- 516 4. A.-S. Chen, T. Taguchi, K. Sakai, Y. Matahira, M.-W. Wang and I. Miwa, *Biol. Pharm.*
517 *Bull.*, 2005, **28**, 1971-1973.
- 518 5. M. S. Azam, E. J. Kim, H.-S. Yang and J. K. Kim, *Springerplus*, 2014, **3**, 1-11.
- 519 6. X. Wu, J. Wang, Y. Shi, S. Chen, Q. Yan, Z. Jiang and H. Jing, *J. Funct. Foods*, 2017,
520 **28**, 96-105.
- 521 7. X. Li, M. Zhao, L. Fan, X. Cao, L. Chen, J. Chen, Y. M. Lo and L. Zhao, *J. Funct.*
522 *Foods*, 2018, **46**, 202-211.
- 523 8. M. Rinaudo, *Prog. Polym. Sci.*, 2006, **31**, 603-632.
- 524 9. Y. S. Nakagawa, V. G. Eijsink, K. Totani and G. Vaaje-Kolstad, *J. Agric. Food*
525 *Chem.*, 2013, **61**, 11061-11066.
- 526 10. E. Husson, C. Hadad, G. Huet, S. Laclef, D. Lesur, V. Lambertyn, A. Jamali, S. Gottis,
527 C. Sarazin and A. N. Van Nhien, *Green Chem.*, 2017, **19**, 4122-4131.
- 528 11. J. Pohling, K. Hawboldt and D. Dave, *Green Chem.*, 2022.
- 529 12. Y. Liu, Z. Jiang, J. Ma, S. Ma, Q. Yan and S. Yang, *J. Agric. Food Chem.*, 2020, **68**,
530 5648-5657.
- 531 13. G. Vaaje-Kolstad, T. R. Tuveng, S. Mekasha and V. G. Eijsink, *Chitin and chitosan:*
532 *properties and applications*, 2019, 189-228.
- 533 14. Y. S. Nakagawa, M. Kudo, R. Onodera, L. Z. P. Ang, T. Watanabe, K. Totani, V. G.
534 Eijsink and G. Vaaje-Kolstad, *J. Agric. Food Chem.*, 2020, **68**, 13641-13650.
- 535 15. J. Li, K. Gao, F. Secundo and X. Mao, *Food Chem.*, 2021, **364**, 130393.
- 536 16. M.-È. Lacombe-Harvey, R. Brzezinski and C. Beaulieu, *App. Microbiol. Biotechnol.*,
537 **2018**, **102**, 7219-7230.
- 538 17. L. Duhsaki, S. Mukherjee, T. S. Rani and J. Madhuprakash, *Environ. Microbiol. Rep.*,
539 **2022**, **14**, 431-442.
- 540 18. N. Nguyen-Thi and N. Doucet, *J. Biotechnol.*, 2016, **220**, 25-32.
- 541 19. B. Nazari, A. Saito, M. Kobayashi, K. Miyashita, Y. Wang and T. Fujii, *FEMS*
542 *Microbiol. Ecol.*, 2011, **77**, 623-635.
- 543 20. A. Saito, H. Ebise, Y. Orihara, S. Murakami, Y. Sano, A. Kimura, Y. Sugiyama, A.
544 Ando, T. Fujii and K. Miyashita, *FEMS Microbiol. Lett.*, 2013, **340**, 33-40.
- 545 21. X. Zhong, L. Zhang, G. P. van Wezel, E. Vijgenboom and D. Claessen, *mBio*, 2022,
546 **13**, e00456-00422.
- 547 22. Y. Kezuka, M. Ohishi, Y. Itoh, J. Watanabe, M. Mitsutomi, T. Watanabe and T.
548 Nonaka, *J. Mol. Biol.*, 2006, **358**, 472-484.
- 549 23. Y. S. Nakagawa, M. Kudo, J. S. Loose, T. Ishikawa, K. Totani, V. G. Eijsink and G.
550 Vaaje-Kolstad, *FEBS J.*, 2015, **282**, 1065-1079.
- 551 24. J. Madhuprakash, N. E. El Gueddari, B. M. Moerschbacher and A. R. Podile, *PLoS*
552 *One*, 2015, **10**, e0116823.
- 553 25. A. Zhang, C. Wang, J. Chen, G. Wei, N. Zhou, G. Li, K. Chen and P. Ouyang, *Green*
554 *Chem.*, 2021, **23**, 3081-3089.
- 555 26. J. Madhuprakash, K. Tanneeru, P. Purushotham, L. Guruprasad and A. R. Podile, *J.*
556 *Biol. Chem.*, 2012, **287**, 44619-44627.
- 557 27. J.-H. Kuk, W.-J. Jung, G.-H. Jo, Y.-C. Kim, K.-Y. Kim and R.-D. Park, *Appl.*
558 *Microbiol. Biotechnol.*, 2005, **68**, 384-389.

559 28. X. Ma, G. Gözaydın, H. Yang, W. Ning, X. Han, N. Y. Poon, H. Liang, N. Yan and K.
560 Zhou, *Proc. Natl. Acad. Sci.*, 2020, **117**, 7719-7728.
561 29. E.-H. Ablouh, R. Jalal, M. Rhazi and M. Taourirte, *Int. J. Biol. Macromol.*, 2020, **151**,
562 492-498.
563 30. N. Nisar, T. Tsuzuki, A. Lowe, J. T. Rossiter, A. Javaid, G. Powell, R. Waseem, S. H.
564 Al-Mijalli and M. Iqbal, *Int. J. Biol. Macromol.*, 2021, **178**, 253-262.
565
566
567
568
569
570
571
572
573
574
575
576
577
578
579
580
581
582
583
584
585
586
587
588
589
590
591
592
593
594
595
596
597
598
599
600
601
602
603
604

605
606 **Table 1:**
607
608

Substrates	I_{110} (~20°)	I_{am} (16°)	I_{CR}
UM α-chitin	52198	6083	88.3%
BM-30	32228	9052	71.9%
BM-60	25711	11170	56.6%

609
610
611
612
613
614
615
616
617

Table 1. Crystallinity Index (C.I.) of the unmilled and ball-milled α -chitin substrates as determined from powder XRD. I_{110} denotes the maximum intensity of diffraction for the (110) plane at $2\theta = 20^\circ$ and I_{am} denotes the intensity of the diffraction at the amorphous region at $2\theta=16^\circ$ approximately.

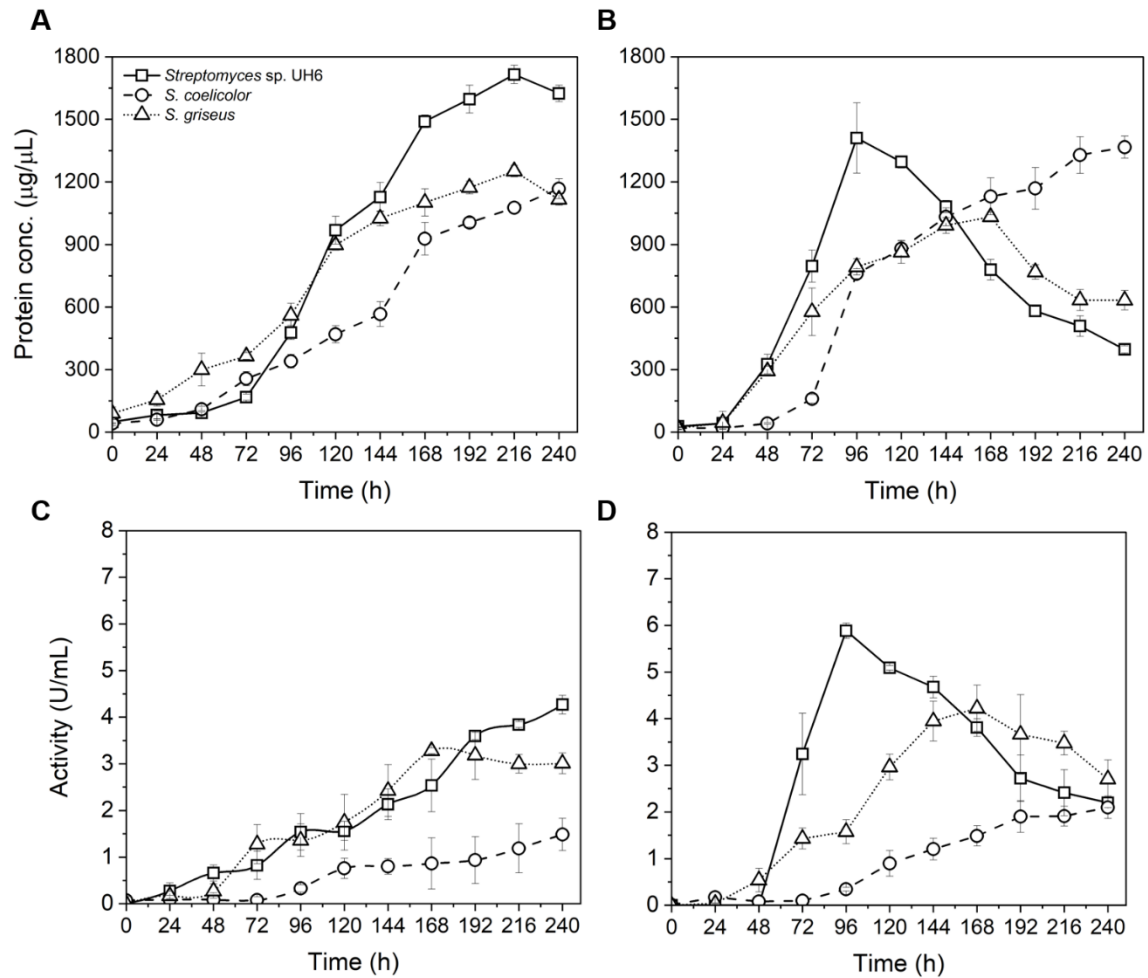
618 **Table 2:**
619
620
621
622

Substrates	S_{BET} (m ² /g)	Fold change of S_{BET}
UM α-chitin	6.3	-
BM-30	10.6	1.69
BM-60	18.6	2.97

623
624
625
626
627
628
629
630
631
632
633
634
635
636
637
638
639

Table 2. S_{BET} analysis of the unmilled and ball-milled α -chitin substrates

640 **Fig. 1:**
641

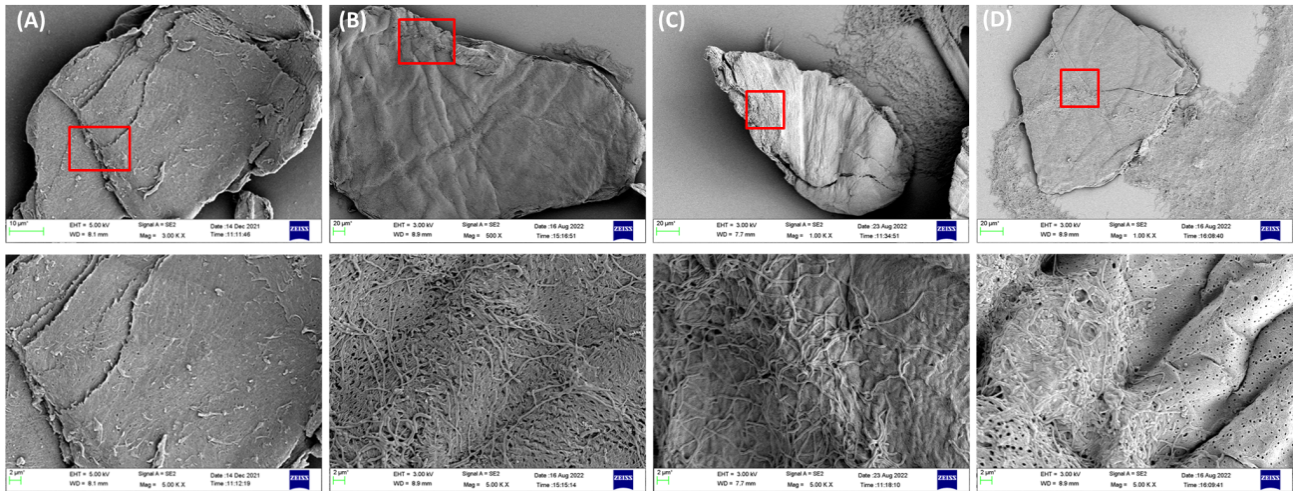


642
643 **Fig. 1.** Cell growth and activity analysis of the *Streptomyces* spp. on α - and β -chitin. Cell
644 growth was analyzed in terms of total cellular protein concentration ($\mu\text{g}/\mu\text{L}$) on α - (A) and β -
645 chitin (B). Extracellular chitinase activity (U/mL) for the secretomes collected over α - (C) and
646 β -chitin (D) was estimated using Schales' assay. The experiment was performed in biological
647 triplicates and error bars represent standard deviation.

648
649
650
651
652
653
654
655
656
657
658
659
660
661

662
663
664

Fig. 2:



665
666
667
668
669
670
671
672
673
674

Fig. 2. FE-SEM micrographs showing the degradation of α -chitin by the *Streptomyces* spp. (A) untreated α -chitin particle; (B, C, D) α -chitin treated with *Streptomyces* sp. UH6, *S. coelicolor* and *S. griseus*, respectively. The upper panel represents the untreated and treated chitin particles, while the lower panel represents the close-up images of the target area (shown in red frame). Scale bar for the images in the upper panel is 20 μm and those in the lower panel is 2 μm .

675 **Fig. 3:**

676

677

678

679

680

681

682

683

684

685

686

687

688

689

690

691

692

693

694

695

696

697

698

699

700

701

702

703

704

705

706

707

708

709

710

711

712

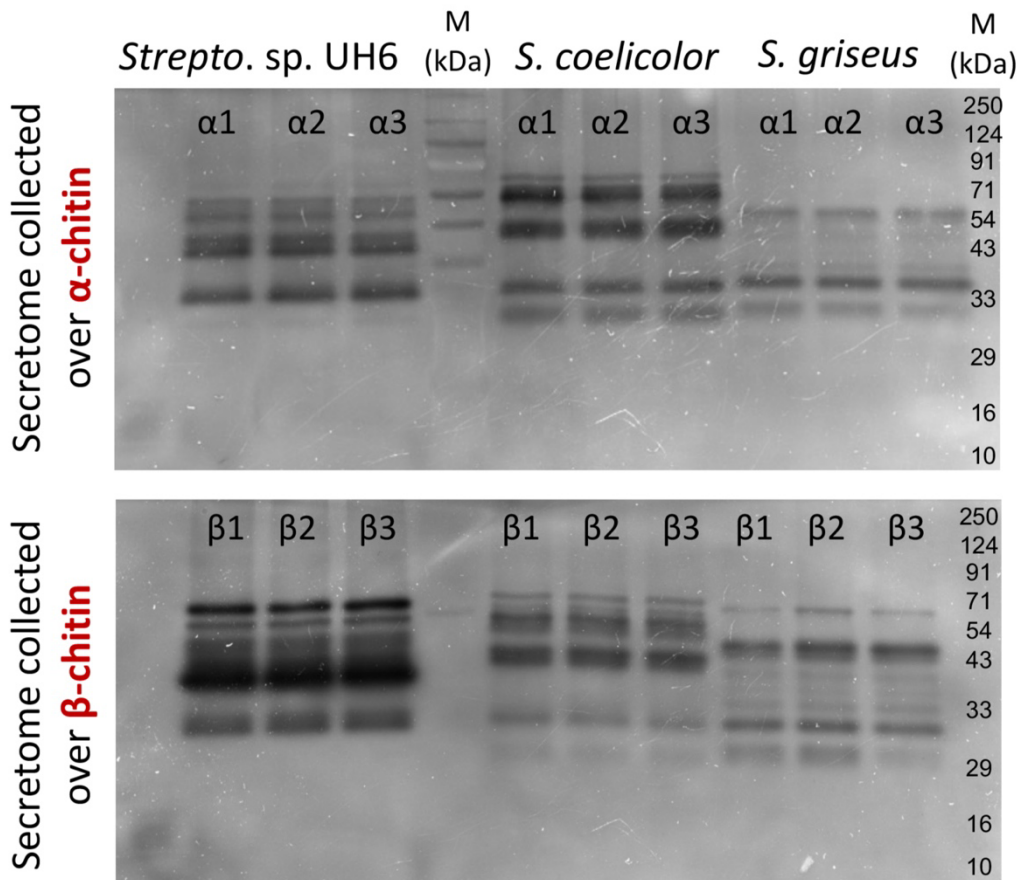
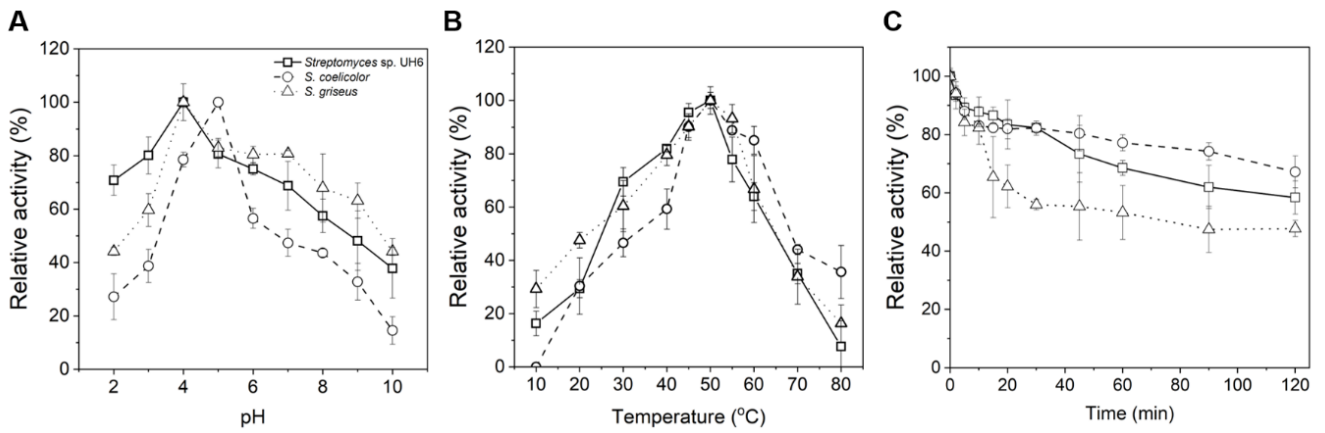


Fig. 3. Semi-native PAGE of *Streptomyces* spp. secretomes using glycol chitin as substrate. Each expression band in the gel is considered as one chitinase isozyme. Upper panel represent chitinase isozymes detected in the secretomes collected over α -chitin, and lower panel represent chitinase isozymes detected in the secretomes collected over β -chitin as substrate. Lanes 1-3, 5-7 and 8-10 represents secretomes produced *Streptomyces* sp. UH6, *S. coelicolor* and *S. griseus*, respectively; lane 4 is protein marker (in kDa) in both panels. The labels $\alpha 1$ -3 and $\beta 1$ -3 represents biological replicates of the secretomes collected over α - and β -chitin, respectively.

713
714 **Fig. 4:**
715

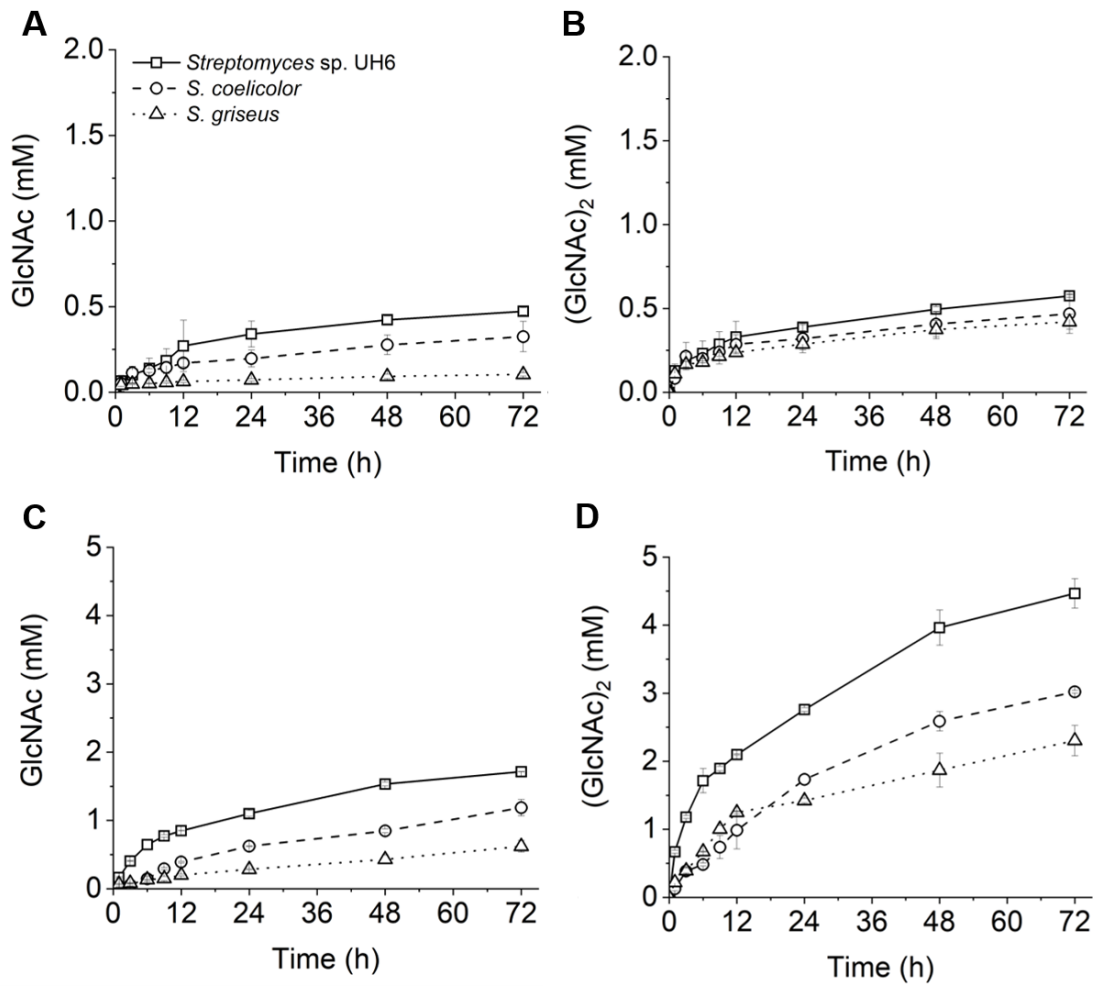


716
717
718 **Fig. 4.** Optimal conditions and thermal stability: (A) Optimal pH of the *Streptomyces*
719 secretomes was measured using different buffers of 50 mM strength at a pH range of 2-10. (B)
720 Optimal temperature was measured at a temperature range of 10-80°C under the optimum pH
721 conditions. (C) The secretomes were pre-incubated at 45°C for different time-intervals and the
722 residual activity was estimated using Schales' assay. All assays were performed in triplicates
723 and error bars indicate standard deviation.

724
725
726

727
728
729

Fig. 5:

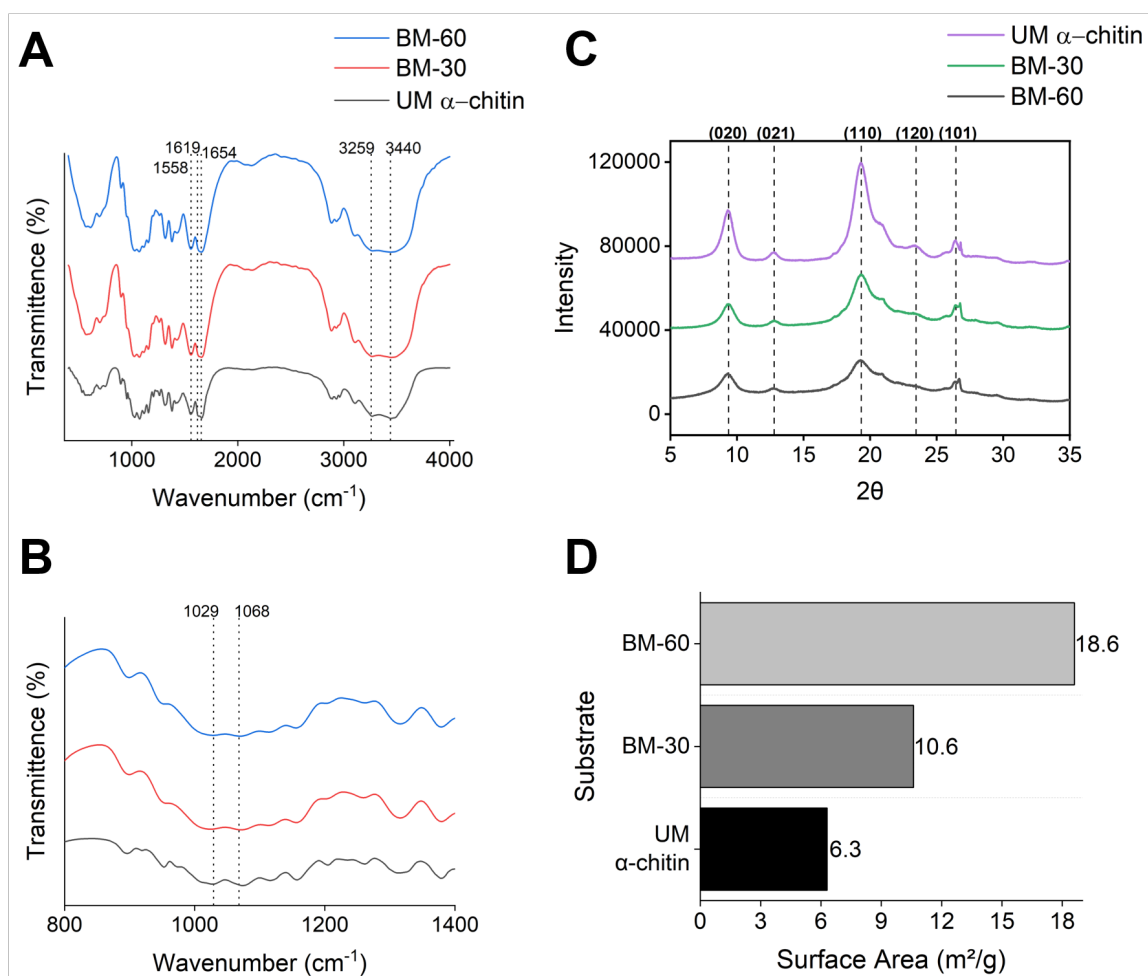


730
731
732
733
734
735
736

Fig. 5. Time-course degradation of α - (A and B) and β -chitin (C and D) by the secretomes produced by *Streptomyces* sp. UH6, *S. coelicolor* and *S. griseus*. All experiments were performed in biological triplicates and the error bars represent standard deviation.

737
738
739
740

Fig. 6:



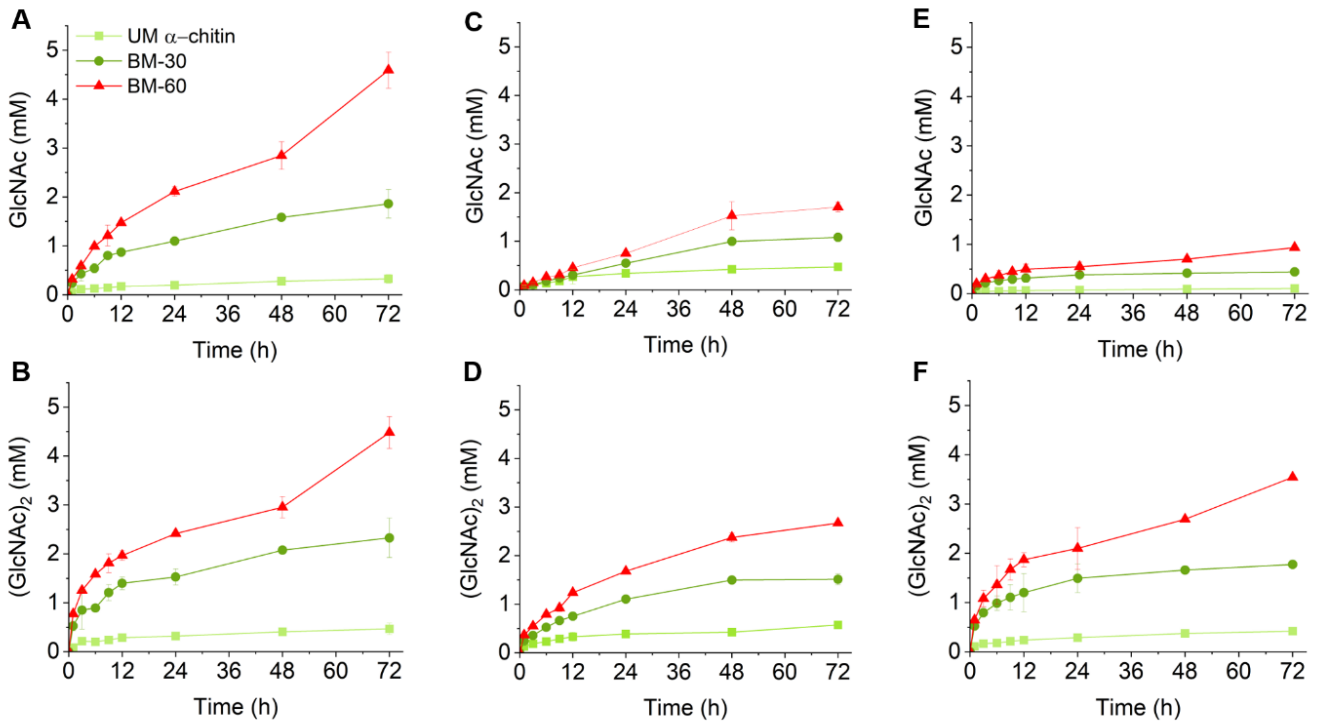
741
742
743
744
745
746
747
748
749

Fig. 6. Characterization of unmilled and ball milled α -chitin substrates by FT-IR (A and B), pXRD (C) and BET analysis (D). UM α -chitin denotes unmilled α -chitin, BM-30 and BM-60 denotes α -chitin ball-milled for 30 and 60 minutes, respectively.

750

751 **Fig. 7:**

752



753

754 **Fig. 7.** A comparative analysis of GlcNAc and (GlcNAc)₂ production from unmilled α -chitin
755 (light green) and the ball-milled α -chitin substrates, BM-30 (green) and BM-60 (red) using
756 chitin-active-secretomes produced by *Streptomyces sp. UH6* (A and B), *S. coelicolor* (C and
757 D) and *S. griseus* (E and F). All experiments were performed in biological triplicates and the
758 error bars represent standard deviation.